Hygrothermal analysis of laminated composites using C^0 FE model based on higher order zigzag theory

S.K. Singh [*1] and A. Chakrabarti [2]

[1] *School of Civil Engineering, Galgotias University, Greater Noida, 201306, U.P., India*
[2] *Department of Civil Engineering, Indian Institute of Technology, Roorkee-247 667, India*

Abstract. A C^0 FE model developed based on an efficient higher order zigzag theory is used for hygrothermal analysis of laminated composite plates. The C^0 FE model satisfies the inter-laminar shear stress continuity at the interfaces and zero transverse shear stress conditions at plate top and bottom. In this model the first derivatives of transverse displacement have been treated as independent variables to circumvent the problem of C^1 continuity associated with the above plate theory. In the present theory the above mentioned C^0 continuity of the present element is compensated in the stiffness matrix formulation by using penalty parameter approach. In order to avoid stress oscillations observed in the displacement based finite element, the stress field derived from temperature/moisture fields (initial strains) must be consistent with total strain field. Special steps are introduced by field consistent approach (e.g., sampling at gauss points) to compensate this problem. A nine noded C^0 continuous isoparametric element is used in the proposed FE model. Comparison of present numerical results with other existing solutions shows that the proposed FE model is efficient, accurate and free of locking.

Keywords: hygrothermal; finite element; zigzag theory; laminated composites; C^0 element

1. Introduction

The composite materials are widely used in civil, aerospace, automobile and other engineering fields due to their advantage of high stiffness and strength to weight ratio. Laminated composite structures are weak in shear due to their low shear modulus compared to extensional rigidity. Therefore, the main attention is given in modeling the shear deformation these types of laminated structures in a refined manner to accurately predict the deflection, stress and other responses. Temperature and moisture concentration are the two important factors which also adversely affect the strength of laminated composite plates. With the increase of temperature and moisture concentrations, the elastic modules and the strength of composite laminate will decrease and sometimes it may be the predominant cause of failure of composite structures.

The analysis of laminated composite structures is more complex in comparison with conventional single-layer structures due to the exhibition of comparatively low value of transverse shear modulus and varying material properties across the thickness of laminates. In view of this situation, various two-dimensional theories, which are simpler and more efficient, compared to 3D elasticity solutions (Tungikar and Rao 1994, Savoia and Reddy 1995, Shankara and Iyengar 1996, Bhaskar *et al.* 1996) have been proposed to study the behaviors of laminates. It is well known that the thermal stresses computed directly from stress-strain and strain-displacement matrices in finite element analysis with simple first-order shear deformation theory shows large errors (Ojalovo 1974, Pittr and Hartl 1980). The results of Lo *et al.* (1977a) have shown subtle discrepancies in the thermal stress analysis of laminated composite plates using C^0 element based on higher-order shear deformation theory for not using consistent and variationally correct formulations (Prathap and Naganarayana 1990, Rama Mohan *et al.* 1994, Prathap and Naganarayana 1995). These errors can be completely removed by consistently reconstituting the thermal strains in the finite element formulation, temperature field used for thermal stress analysis must have the same consistency as the element strain fields and if element stresses are computed at gauss points, the thermal stresses must also be based on these gauss points (Prathap and Naganarayana 1990, 1995, Rama Mohan *et al.* 1994). This strategy evolved from the understanding that the unreliable stress predictions originate from the mismatch between the usual element strain and initial (e.g., hygrothermal) strain. One can show that this is due to the lack of consistency of their respective interpolations within the element.

Naganarayana *et al.* (1995) showed that stress resultant field computed from strain fields in a displacement-type finite element description of domain with sectional rigidities shows extraneous oscillations. This condition arises from the fact that stress resultant fields were of higher interpolation order than the strain fields. Hence higher degree stress resultant terms did not participate in the stiffness matrix calculations. In order to remove the oscillations, a consistent stress resultant field must be derived before stress resultant calculations are performed.

∗Corresponding author, Ph.D.,
  E-mail: sushilbit@yahoo.co.in

Naganarayana *et al.* (1997) demonstrated that consistent formulations give the variationally correct solutions for all types of problem.

Rolfes *et al.* (1998) has presented analytical solution based on the first order shear deformation theory for the evaluation of the transverse thermal stresses in laminated plates. Ali *et al.* (1999) employed displacement based higher-order theory for any combination of mechanical and thermal loading in case of symmetric laminates. Makhecha *et al.* (2001) employed new displacement based higher-order theory for dynamic analysis of laminated composite plates subjected to thermal/mechanical loading. Patel *et al.* (2002) studied the static and dynamic characteristic of thick laminates exposed to hygrothermal environment using a realistic higher-order theory. Khare *et al.* (2003) developed closed form solution based on higher-order shear deformation theory for the thermo-mechanical analysis of simply supported doubly curved cross-ply laminated shell. Kapuria and Achary (2004) presented a new zigzag theory based on zigzag third-order variation of in-plane displacements for laminated plates subjected to thermal loading. Matsunaga (2004) evaluated interlaminar stresses and displacements in cross-ply multilayered composite and sandwich plates subjected to thermal loadings using two-dimensional global higher-order deformation theory. Wang *et al.* (2005) studied the response of dynamic interlaminar stresses in laminated composite plates with piezoelectric layers using an analytical approach based on the layer wise theories.

Wu and Chen (2006) presented global-local higher order shear deformation theory which satisfies the free surface conditions and the geometric and stress continuity conditions at interfaces for angle ply laminated plates. Wu *et al.* (2007) proposed global-local higher order model considering transverse normal deformation to predict the thermal response of laminated plates subjected to actual temperature field. These models give good results for deflection as well as stresses but some unknown parameters are used in the formulations which have no physical meaning and should be avoided in a practical analysis. Bahrami and Nosier (2007) developed elasticity formulation for the displacement field of a long generally stacked laminate subjected to hygrothermal loads. Oh and Cho (2007) presented a higher order zigzag shell theory to predict the mechanical, thermal and electric response of smart laminates. Kant *et al.* (2008) proposed a semi analytical model based on solution of a two-point boundary value problem through the thickness of the plate for thermo-mechanical stress analysis. Brischetto and Carrera (2010) considered a fully coupled thermo-mechanical analysis of one-layered and multilayered isotropic and composite plates. Lo *et al.* (2010) studied the response of laminated composite plates due to variation in temperature and moisture concentrations based on global-local higher-order shear deformation theory. Singh and Chakrabarti studied the hygrothermal analysis of laminated composite plates by using efficient higher order shear deformation theory. In the present formulation, the plate model has been implemented with a computationally efficient C^0 finite element developed by using consistent strain field. But C^1 continuities are required in the transverse displacement functions as the first and second derivatives are involved in the computation of the strain components. Brischetto (2012) analyzed the bending of multilayered composite plates under hygro-thermal loading conditions. Refined two-dimensional models are used to evaluate these effects. Such loads can be determined via a priori linear or constant moisture content and temperature profiles through the thickness of the plate. Topal (2013) studied the response of a new extended layerwise optimization method for thermal buckling load optimization of laminated composite plates. Brischetto (2013) proposed the refined two-dimensional models for the static hygrothermoleastic analysis of multilayered composite and sandwich shells. The design objective is the maximization of the critical thermal buckling of the laminated plates. Kaci *et al.* (2014) studied the nonlinear cylindrical bending of an exponential functionally graded plate (simply called E-FG) with variable thickness. The plate is subjected to uniform pressure loading and his geometric nonlinearity is introduced in the strain-displacement equations based on Von-Karman assumptions. Hadji *et al.* (2014) developed higher order shear deformation theory static and free vibration analysis of functionally graded beams. Nguyen *et al.* (2015) presented refined higher-order shear deformation theory for bending, vibration and buckling analysis of functionally graded sandwich plates. It contains only four unknowns, accounts for a hyperbolic distribution of transverse shear stress and satisfies the traction free boundary conditions. Ebrahimi and Habibi (2016) utilized the finite element method to predict the deflection and vibration characteristics of rectangular plates made of saturated porous functionally graded materials (PFGM) within the framework of the third order shear deformation plate theory. Material properties of PFGM plate are supposed to vary continuously along the thickness direction according to the power-law form and the porous plate is assumed of the form where pores are saturated with fluid.

Pandit *et al.* (2008) developed a C^0 FE model for the analysis of soft core sandwich laminates with unknown nodal parameters, which have physical meaning. Pandit *et al.* (2008) used quadratic variation of transverse displacement across the soft core while it is considered constant for the top and bottom face sheets. But the application of this model is limited to sandwich plates with single core only. Moreover, for composite and sandwich laminates (without very soft core) there is hardly any variation of transverse displacement across the thickness. In the present paper an improved C^0 FE model has been developed based on an efficient higher order zigzag theory to study the static response of laminated composite plates exposed to hygrothermal environment. In this model the transverse displacement has been considered constant across the thickness which simplifies the formulation and reduces the number of nodal unknowns. This also helps to increase the range of applicability of the proposed FE model to different problems of laminated and sandwich plates. In this model the first derivatives of transverse displacement have been treated as independent variables to overcome the problem of C^1 continuity associated with the plate theory. The C^0

continuity of the present element has been compensated in stiffness matrix by using penalty parameter approach. Stress oscillations observed in the displacement based finite element is eliminated by consistently reconstituting the thermal strains in the finite element formulation (Prathap and Naganarayana 1990, 1995, Rama Mohan *et al.* 1994). Special steps were introduced following the field consistent approach (e.g., sampling at gauss points) to compensate this problem. A nine noded C^0 continuous isoparametric element is used to model the proposed theory.

2. Formulation

The in-plane displacement fields are taken as below

$$u_\alpha = u^0{}_\alpha + \sum_{k=0}^{nu-1} S^k{}_\alpha \, (Z - Z_k) H(Z - Z_k)$$
$$+ \sum_{k=0}^{nl-1} T^k{}_\alpha \, (Z - \rho_k) H(-Z + \rho_k) + \xi_\alpha Z^2 + \varphi_\alpha Z^3 \tag{1}$$

where u^0_α denotes the in-plane displacement of any point on mid surface, n_u and n_l represent number of upper and lower layers respectively, S^k_α, T^k_α are the slopes of k-th layer corresponding to upper and lower layers respectively, ξ_α, φ_α are the higher order unknown terms, $H(Z - Z_k)$, $(Z - \rho_k)$ are unit step functions and the subscript α represents the co-ordinate directions [$\alpha = 1, 2$, i.e., x, y in this case respectively and

$$u_3 = w(x, y) \tag{2}$$

The stress –strain relationship of a lamina, say k^{th} lamina having any fiber orientation with respect to structural axes system (x-y-z) may be expressed as

$$\overline{\sigma} = \overline{[Q_k]}\{\overline{\varepsilon}\} \tag{3}$$

The rigidity matrix $\overline{Q_k}$ can be evaluated by material properties and fibre orientation following usual techniques for laminated composites.

Now by utilizing the transverse shear stress free boundary condition at the top and bottom of the plate, $\sigma_{3\alpha|z=\pm h/2} = 0$ the components ξ_α and φ_α could be expressed as

$$\Phi_\alpha = -\frac{4}{3h^2}\left\{ w,_\alpha + \frac{1}{2}\left(\sum_{k=0}^{nu-1} S_\alpha^K + \sum_{k=0}^{n_{l}-1} T_\alpha^k\right)\right\} \tag{4}$$

and

$$\xi_\alpha = -\frac{1}{2}\left(\sum_{k=0}^{nu-1} S_\alpha^k - \sum_{k=0}^{nl-1} T_\alpha^k\right) \tag{5}$$

Similarly by imposing the transverse shear stress continuity conditions at the layer interfaces the following expressions for S_α and T_α are obtained as below

$$S_\alpha^k = a_{\alpha\gamma}^k\left(w,_\gamma + \Psi_\gamma\right) + b_{\alpha\gamma}^k \, w,_\gamma \tag{6}$$

$$T_\alpha^k = c_{\alpha\gamma}^k\left(w,_\gamma + \Psi_\gamma\right) + d_{\alpha\gamma}^k \, w,_\gamma \tag{7}$$

where $a_{\alpha\gamma}^k$, $b_{\alpha\gamma}^k$, $c_{\alpha\gamma}^k$, $d_{\alpha\gamma}^k$ are constants depending on material and geometric properties of individual layers, $w,_\gamma$ is the derivatives of transverse displacement while $\gamma = 1, 2$ and $S_\alpha^0 = \Psi_\alpha$ is the rotation of normal at the mid surface about co-ordinate directions [$\alpha = 1, 2$, i.e., x, y in this case].

By using Eqs. (2)-(6) the strain vector can be evaluated by

$$\{\overline{\varepsilon}\}_{5\times1} = [H]_{5\times17}\{\varepsilon\}_{17\times1} \tag{8}$$

$\{\overline{\varepsilon}\}$ is the strain field vector and $\{\varepsilon\}$ is the strain vector at the reference plane (i.e., at the mid plane) where the $[H]$ matrix consists of terms containing z and some term related to material properties.

In order to avoid the difficulties associated with C^1 continuity the derivatives of w with respect to x and y are expressed as follows

$$w,_1 = \frac{\partial w}{\partial x} = w_1 \text{ and } w,_2 = \frac{\partial w}{\partial y} = w_2 \tag{9}$$

which helps to define all the variables as C^0 continuous.

$$\{\varepsilon\}^T$$
$$= \left\{ \begin{array}{l} \frac{\partial u_1^0}{\partial x} \; \frac{\partial u_2^0}{\partial y} \; \frac{\partial u_2^0}{\partial x} + \frac{\partial u_1^0}{\partial y} \; \frac{\partial w_1}{\partial x} \; \frac{\partial w_2}{\partial y} \; \frac{\partial w_2}{\partial x} \; \frac{\partial w_1}{\partial y} \; \frac{\partial \Psi_1}{\partial x} \; \frac{\partial \Psi_2}{\partial y} \\[2mm] \frac{\partial \Psi_2}{\partial x} \; \frac{\partial \Psi_1}{\partial y} \; \Psi_1 \; \Psi_2 \; \frac{\partial w}{\partial x} \; \frac{\partial w}{\partial y} \; w_1 \; w_2 \end{array} \right\} \tag{10}$$

The strain displacement relation may be written as below

$$\{\varepsilon\} = [B]\{\delta\} \tag{11}$$

here $[B]$ is the strain-displacement matrix and $\{\delta\}$ is the element nodal unknown vector.

Thermal strain due to temperature change is be given by

$$\{\varepsilon_{th}\} = \left\{ \begin{array}{c} \alpha_x \Delta T \\ \alpha_y \Delta T \\ \alpha_{xy} \Delta T \\ \gamma_{xz} \\ \gamma_{yz} \end{array} \right\} \tag{12a}$$

in which ΔT is the change of temperature/moisture concentration with respect to reference temperature concentration, $\alpha_x, \alpha_y, \alpha_{xy}$ are the thermal expansion coefficients in the structural axis (x-y-z) system

Moisture (i.e., hygro) strain due to moisture change is be given by

$$\{\varepsilon_m\} = \left\{ \begin{array}{c} \beta_x \Delta M \\ \beta_y \Delta M \\ \beta_{xy} \Delta M \\ \gamma_{xz} \\ \gamma_{yz} \end{array} \right\} \tag{12b}$$

in which ΔM is the change of moisture concentration with respect to reference moisture concentration, $\beta_x, \beta_y, \beta_{xy}$ are the moisture expansion coefficients in the structural axis (x-y-z) system

Therefore, the net strain may be written as

$$\{\overline{\varepsilon}_n\} = \{\overline{\varepsilon}\} - \{\varepsilon_{th}\} \tag{13a}$$

$$\{\bar{\varepsilon}_n\} = \{\bar{\varepsilon}\} - \{\varepsilon_m\} \tag{13b}$$

in which $\{\bar{\varepsilon}_n\}$ is the total strain and $\{\varepsilon_{th}\}$ is the thermal strain/$\{\varepsilon_m\}$ is the moisture strain respectively.

For the present study, a nine noded C^0 continuous isoparametric element shown in Fig. 2 with seven unknowns (i.e., u_1, u_2, w, Ψ_1, Ψ_2, w_1, w_2) are used to develop the proposed finite element model. The generalized displacements included in the present theory can be expressed as follows

$$u_1 = \sum_{i=1}^{9} N_i u_i, \quad u_2 = \sum_{i=1}^{9} N_i v_i,$$

$$w = \sum_{i=1}^{9} N_i w_i, \quad \Psi_1 = \sum_{i=1}^{9} N_i \Psi_{1_i},$$

$$\Psi_2 = \sum_{i=1}^{9} N_i \Psi_{2_i}, \tag{14}$$

$$w_1 = \sum_{i=1}^{9} N_i w_{1_i}, \quad w_2 = \sum_{i=1}^{9} N_i w_{2_i}$$

where N_i are the shape functions for the nine noded isoparametric element.

By applying virtual work method

$$[k]\{\delta\} = \{P\} \tag{15}$$

where $[k]$ is the element stiffness matrix and $\{P\}$ is the element nodal load vector as written below

$$[k] = \iint [B]^T [D][B] dx dy \tag{16}$$

where $[B]$ is the strain displacement matrix and $[D]$ is the rigidity matrix respectively.

$$\{P\} = \iint [N]^T q dx dy \tag{17}$$

where $[N]$ is the shape functions matrix and q is the intensity of transverse load respectively.

Thermal loading may be obtained as below

$$\{F\} = \iint [B]^T [H]^T \{F^N\} dx dy \tag{18}$$

where $\{F^N\}^T = \left[N_x{}^N, N_y{}^N, N_{xy}{}^N, \text{etc} - - - \right]$ and $\{F\}$ is the thermal load respectively.

And

$$\{N_x{}^N, N_x{}^N, N_{xy}{}^N\}^T = \sum_{k}^{n} \int_{z_{k-1}}^{z_k} \{\bar{Q}_{ij}\}_k \{\varepsilon_{th}\} dz \tag{19}$$

here $i, j = 1, 2, 6$ and $\{\varepsilon_{th}\}$ is the thermal strain components.

It can be observed that the total strain field is always interpolated to a lower order when compared to the thermal strain fields. Hence thermal strain fields should be consistently reconstituted to the order of in-plane normal strain field to get accurate strains and stresses over the element domain. Therefore, this is accordingly taken care to

make them field consistent (Noor and Burton 1992).

The following thermal cases are considered:

Case 1 (a): Temperature uniform across the depth

$$\begin{Bmatrix} \varepsilon_x \\ \varepsilon_y \\ \varepsilon_{xy} \end{Bmatrix} = \begin{Bmatrix} \alpha_x \\ \alpha_y \\ \alpha_{xy} \end{Bmatrix} . \Delta T \tag{20a}$$

$$\begin{Bmatrix} \alpha_x \\ \alpha_y \\ \alpha_{xy} \end{Bmatrix} = \begin{bmatrix} c^2 & s^2 & -2cs \\ s^2 & c^2 & 2cs \\ cs & -cs & c^2 - s^2 \end{bmatrix} [Q]_k \begin{Bmatrix} \alpha_1 \\ \alpha_2 \\ \alpha_{12} \end{Bmatrix}_k \tag{20b}$$

where $\alpha_1, \alpha_2, \alpha_{12}$ are thermal expansion coefficient in the material axis system and $c = \cos\theta$, $s = \sin\theta$ and θ is the angle between principal material axis and structural axis system.

In this case, $\Delta T = T$, therefore, thermal force

$$\{F\} = \iiint [B]^T [H]^T \begin{Bmatrix} \alpha_x \\ \alpha_y \\ \alpha_{xy} \end{Bmatrix} . T dv \tag{21}$$

Case 1 (b): Moisture uniform across the depth

$$\begin{Bmatrix} \varepsilon_x \\ \varepsilon_y \\ \varepsilon_{xy} \end{Bmatrix} = \begin{Bmatrix} \beta_x \\ \beta_y \\ \beta_{xy} \end{Bmatrix} . \Delta T \tag{22a}$$

$$\begin{Bmatrix} \beta_x \\ \beta_y \\ \beta_{xy} \end{Bmatrix} = \begin{bmatrix} c^2 & s^2 & -2cs \\ s^2 & c^2 & 2cs \\ cs & -cs & c^2 - s^2 \end{bmatrix} [Q]_k \begin{Bmatrix} \beta_1 \\ \beta_2 \\ \beta_{12} \end{Bmatrix}_k \tag{22b}$$

where $\beta_1, \beta_2, \beta_{12}$ are moisture expansion coefficient in the material axis system and $c = \cos\theta$, $s = \sin\theta$ and θ is the angle between principal material axis and structural axis system.

In this case, $\Delta M = M$, therefore, Hygro(moisture) force

$$\{F\} = \iiint [B]^T [H]^T \begin{Bmatrix} \beta_x \\ \beta_y \\ \beta_{xy} \end{Bmatrix} . M dv \tag{23}$$

Case 2(a): Temperature varying across the depth, therefore, thermal force

$$\{F\} = \iiint [B]^T [H]^T \begin{Bmatrix} \alpha_x \\ \alpha_y \\ \alpha_{xy} \end{Bmatrix} . \\ [1/2(T_U + T_L + z/h(T_U - T_L)] . dv \tag{24a}$$

where, T_U = Temperature at top surface
T_L = Temperature at bottom surface

Case 2(b): Moisture varying across the depth, therefore, Moisture force

$$\{F\} = \iiint [B]^T [H]^T \begin{Bmatrix} \beta_x \\ \beta_y \\ \beta_{xy} \end{Bmatrix} . \\ [1/2(M_U + M_L + z/h(M_U - M_L)] . dv \tag{24b}$$

where, M_U = Moisture at top surface
M_L = Moisture at bottom surface

Once the element stiffness matrix and the element load vector are formed, the corresponding global matrices can also be formed by following a standard assembly operation. After incorporation of suitable boundary conditions, the problem of linear simultaneous equations is solved to get the nodal unknowns and therefore the stresses at different locations.

3. Results and discussion

In order to demonstrate the accuracy of the present C^0 finite element model, a numerical code has been developed in FORTRAN language. A number of numerical examples with different temperature/moisture variations have been solved considering different features such as boundary conditions, ply orientations, thickness ratio and aspect ratio. The results obtained by using the proposed FE model is first validated with some published results and then many new results are also generated. The convergence of the proposed FE results is also studied in the first example.

3.1 Cross-ply $(0^0/90^0/0^0)$ composite plate simply supported at all the edges

In this example static response of laminated square composite plate has been analyzed subjected to equal rise and fall of temperature respectively at the top and bottom surface of the plate (to ensure pure bending) with sinusoidal in-plane variations. The material properties of individual layers are given by: $E_1/E_2 = 25$, $G_{12} = G_{13} = 0.5E_2$, $G_{23} = 0.2E_2$, $v_{12} = v_{13} = 0.25$, $\alpha_2/\alpha_1 = 1125$.

$$T = T_U \, \text{SIN} \, (\pi X/a)\text{SIN} \, (\Pi x/b) \text{ (for Upper layer)}$$

$$T = T_L \, \text{SIN} \, (\pi X/a)\text{SIN} \, (\Pi x/b) \text{ (for lower layer)}$$

Where T_U = Temperature of upper layer

T_L = Temperature of lower layer
a = length of plate
b = width of plate

The deflection and stresses are presented in terms of following non-dimensional parameters: $\overline{w} = \frac{w}{h\alpha_1 T_0 S^2}$, $(\overline{u}, \overline{v}) = \frac{(u,v)}{h\alpha_1 T_0 S}$, $(\overline{\sigma}_i, \overline{\tau}_{ij}) = \frac{(\sigma_i, \tau_{ij})}{E_1 \alpha_1 T_0}$.

3.1.1 Transverse deflections and in-plane stresses for simply supported cross ply $(0^0/90^0/0^0)$ square laminate

This problem is solved to assess the performance of the proposed C^0 plate element with the same temperature loadings mentioned above. The thickness ratio (a/h) is taken 100 where a is the planar dimension of the plate in x-direction and h is the overall thickness of the plate. The convergence of the non-dimensional transverse deflection and in-plane stresses obtained by using the proposed element is shown in Table 1. The transverse deflection and the in-plane normal stresses are calculated at the midpoint $(x = a/2$ and $y = a/2)$ of the plate while for in-plane shear it is calculated at the corner of the plate $(x = 0$ and $y = 0)$ at

Table 1 Non-dimensional transverse deflections and in-plane stresses for simply supported cross ply $(0^0/90^0/0^0)$ square laminate $(a/h = 100)$

References	$\overline{w}$	$\overline{\sigma}_X$	$\overline{\sigma}_y$	$\overline{\tau}_{xy}$
Present (4×4^1)	10.03	950.90	1067.13	53.84
Present (6×6)	10.21	972.69	1064.49	51.71
Present (8×8)	10.21	971.46	1064.05	50.97
Present (12×12)	10.21	967.80	1064.15	50.49
Present (16×16)	10.20	965.09	1064.31	50.27
Bhaskar (1996)	10.26	965.40	1065.00	50.53

[1] Mesh division

Table 2 Non-dimensional in-plane and transverse displacements for simply supported cross-ply $(0^0/90^0/0^0)$ square laminate

Thickness ratio (a/h)	References	$\overline{u}$	$\overline{v}$	$\overline{w}$
100	Present(16×16)	16.08	16.00	10.20
	Bhaskar (1996)	16.00	16.17	10.26
50	Present(16×16)	16.34	16.27	10.37
	Bhaskar (1996)	16.02	16.71	10.50
20	Present(16×16)	17.98	17.90	11.41
	Bhaskar (1996)	16.17	20.34	12.12
10	Present(16×16)	22.98	22.90	14.57
	Bhaskar (1996)	16.60	31.92	17.37

thickness, z = ± h/2. It is found that with refining meshes (16 × 16, full plate) the present finite element results closely match with the results of 3D elasticity solution of Bhaskar *et al.* (1996).

3.1.2 In-plane and transverse displacements for simply supported cross-ply $(0^0/90^0/0^0)$ square laminate

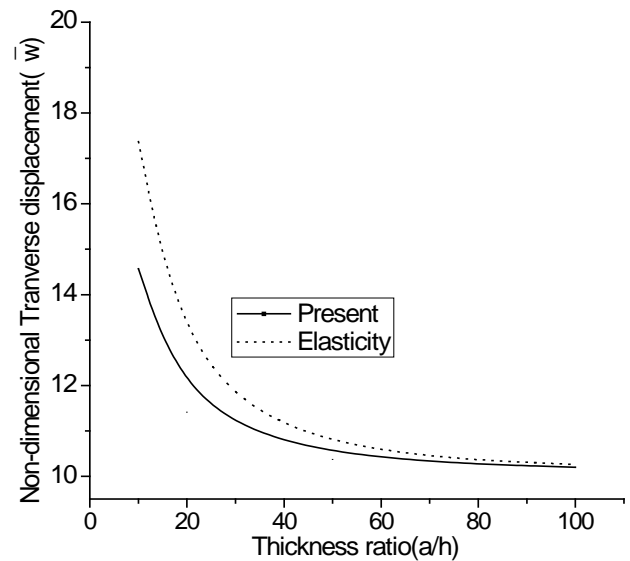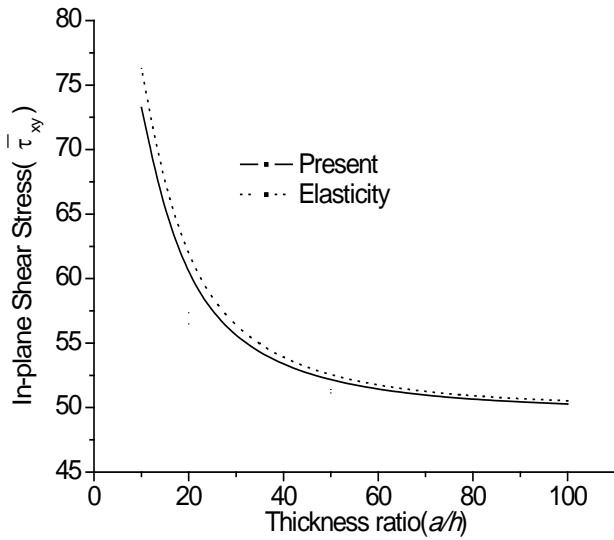The effect of thickness ratio (a/h) has been studied in

Fig. 1 Variation of of non-dimensional transverse displacement $(\overline{w})$ for cross ply $(0^0/90^0/0^0)$ square laminate for different thikness ratio

Table 3 Non-dimensional stresses for simply supported $(0^0/90^0/0^0)$ square laminate

Thickness ratio (a/h)	References	$\overline{\sigma}_X$	$\overline{\sigma}_y$	$\overline{\tau}_{xy}$	$\overline{\tau}_{xz}$	$\overline{\tau}_{yz}$
10000	Present (16×16)	312.80	1127.32	0.09	0.02	0.06
1000	Present (16×16)	1501.45	875.47	27.85	0.23	0.42
100	Present (16×16)	965.09	1064.31	50.27	6.48	6.31
	Bhaskar (1996)	965.40	1065.00	50.53	7.07	7.08
50	Present (16×16)	967.59	1062.00	51.14	12.89	12.50
	Bhaskar (1996)	967.5	1063.00	51.41	14.07	14.13
20	Present (16×16)	971.45	1052.06	56.49	31.16	30.40
	Kant (2008)	982.00	1051.24	57.48	-	-
	Bhaskar (1996)	982.00	1051.00	57.35	33.98	34.76
10	Present (16×16)	978.01	1018.41	73.25	55.67	55.99
	Kant (2008)	1026.3	1014.36	76.29	-	-
	Bhaskar (1996)	1026	1014.00	76.29	60.54	66.01

Fig. 2 Variation of non dimensional in-plane stress ($\overline{\tau}_{xy}$) the cross-ply $(0^0/90^0/0^0)$ laminated square plate with different thickness ratio

been studied on the values of non-dimensional in-plane stresses and transverse shear stresses considering very thin to moderately thick plates. In-plane normal stresses are calculated at the midpoint ($x = a/2$ and $y = a/2$), in-plane shear stress is calculated at the corner of the plate ($x = 0$ and $y = 0$) while out of plane shear stresses, $\overline{\tau}_{xz}$ at $(0, a/2)$ and $\overline{\tau}_{yz}$ at $(a/2, 0)$ at thickness, $z = \pm h/6$. The corresponding results are presented in Table 3 along with the other results. The present finite element results are very close to results of 3D elasticity solution of Bhaskar *et al.* (1996).

The non-dimensional in-plane shear stress ($\overline{\tau}_{xy}$) has been plotted in Fig. 2. The results of the 3D elasticity solution of Bhaskar *et al.* (1996) are also plotted on the same figures. The comparison between the results clearly indicates that the present results are very close to the results of 3D elasticity solution of Bhaskar *et al.* (1996).

3.2 Cross-ply $(0^0/90^0)$ composite plate simply supported at all the edges

In this section, the example of a two layered cross ply $(0^0/90^0)$ square composite plate with equal thickness of the

Table 4 In-plane displacements and Transverse displacement of two layered $(0^0/90^0)$ simply supported square laminate

Thickness ratio (a/h)	References	u	v	w
100	Present (16×16)	0.1714	0.1054	5.9427
	Brischetto and Carrera (2010)	0.1747	-	5.9448
50	Present (16×16)	0.0852	0.05354	1.4850
	Brischetto and Carrera (2010)	0.0882	-	1.4857
10	Present (16×16)	0.0144	0.0127	0.0586
	Brischetto and Carrera (2010)	0.0225	-	0.0587
5	Present (16×16)	0.0045	0.0137	0.0141
	Brischetto and Carrera (2010)	0.0171	-	0.0141

the present problem considering very thin to moderately thick plates with the same temperature loading. The non-dimensional in-plane displacements $\overline{u}$ (at $x = 0$, $y = a/2$) and $\overline{v}$ (at $x = a/2$, $y = 0$); and the non-dimensional transverse deflection, $\overline{w}$ (at $x = a/2$, $y = a/2$) at thickness, $z = \pm h/2$ are calculated by using the present FE model and the results are as shown in Table 2. The variation of non-dimensional transverse-displacement ($\overline{w}$) with different thickness ratio (a/h) has been plotted in Fig. 1. The results of the 3D elasticity solution Bhaskar *et al.* (1996) are also plotted on the same figure. It is observed that the present results are quite close to the results of 3D elasticity solution of Bhaskar *et al.* (1996) for higher thickness ratio ($a/h = 100$) where as for lower thickness ratio, there are slight variations between the results.

3.1.3 In-plane and transverse stresses for simply supported $(0^0/90^0/0^0)$ square laminate

In the present problem the effect of thickness ratio has

Table 5 Non-dimensional transverse displacement ($\overline{w}$) of simply supported rectangular laminate for different aspect ratio (a/b)

a/h	References	$0^0/90^0/0^0$			$0^0/90^0$		
		$a/b = 1$	$a/b = 1.5$	$a/b = 2$	$a/b = 1$	$a/b = 1.5$	$a/b = 2$
100	Present(16×16)	1.0282	0.8764	0.6477	1.1382	0.5129	0.2690
	GPrathap (1995)	1.0249	0.8802	0.6566	1.1434	-	-
	Nastran (1995)	1.0028	0.8346	0.6108	1.1374	-	-
10	Present(16×16)	1.0510	0.8536	0.5978	1.1424	0.5465	0.2794
5	Present(16×16)	1.0866	0.8201	0.5486	1.1244	0.5622	0.2875

* $\overline{w} = 10hw/\alpha_1 T_0 \alpha_2$

individual layers subjected to imposed temperature, $\theta_t = 1.0$ K at the top and $\theta_b = 0.0$ K. at the bottom surfaces of the plate with sinusoidal in–plane variations has been considered. The material properties of individual layers are given by

$$E_1 = 172.72 \text{ GPa}, \qquad E_2 = E_3 = 6.909 \text{ GPa},$$

$$G_{12} = G_{13} = 3.45 \text{ GPa}, \qquad G_{23} = 1.38 \text{ GPa}, \qquad v_{12} = 0.25$$

Results of maximum in-plane displacements (u, v in mm) and transverse displacement (w in mm) are presented in Table 4 for various thickness ratios. The present results of in-plane displacement (u) and transverse displacement (w) match closely with the results of Brischetto and Carrera (2010).

3.3 Effect of aspect ratio, number of plies and their orientations

In this section the effect of aspect ratio, number of plies and their orientations is studied on non-dimensional deflection, $\overline{w}$ for simply supported laminated plate (thickness ratios, $a/h = 100$, 10 and 5) subjected to same temperature variation as taken in the previous section. The material properties are as given below.

$$E_1/E_2 = 25 \qquad G_{12}/E_2 = 0.5 \qquad G_{23}/E_2 = 0.2 \qquad v_{12} = 0.25$$

$$G_{12} = G_{13} \qquad \text{and} \qquad v_{12} = v_{13}, \alpha_2 = 3\alpha_1$$

The non-dimensional ($\overline{w}$) displacements obtained by

using the proposed FE model are presented in Table 5 with those obtained by Prathap and Naganarayana (1995) and by using the standard software MSC/NASTRAN (1995). The results obtained by the proposed FE model are quite close to the above results Prathap and Naganarayana (1995). Some new results are also generated.

3.4 Effect of different boundary conditions

The influence of different boundary conditions on non-dimensional transverse displacement and in-plane stresses is investigated in the present section. The plate is considered simply supported (S) along the edges parallel to the y axis while the other edges have simply supported (S), clamped (C) or free (F) boundary conditions. The notation SSCF, for example refers to the simply supported boundary conditions of the two edges parallel to the y- axis and the clamped and free conditions for the two edges parallel to the x- axis. In this example, non-dimensional transverse displacement and in-plane stresses of square laminated composite plate has been analyzed subjected to equal rise and fall of temperature at the top and bottom surfaces of the plate with sinusoidal in-plane variations. The material properties used are as given below.

$$E_1/E_2 = 40 \qquad G_{12}/E_2 = 0.6 \qquad G_{23}/E_2 = 0.5 \qquad v_{12} = 0.25$$

$$G_{12} = G_{13} \quad \text{and} \quad v_{12} = v_{13}, \qquad \alpha_2 = 1125\alpha_1$$

The deflection and stresses are presented in terms of following non-dimensional parameters

Table 6 Non-dimensional transverse displacements and in-plane stresses for square laminate ($0^0/90^0/0^0/90^0$) under different boundary conditions

Thickness ratio	References	Boundary conditions	$\overline{w}$	$\overline{\sigma}_x$	$\overline{\sigma}_y$	$\overline{\tau}_{xy}$
100	Present (16×16)	SSSS	8.6920	237.5057	271.2219	14.7584
	Present (16×16)	SSCC	3.2899	2.3138	277.7459	2.1941
	Present (16×16)	SSFF	8.9194	45.3909	271.5353	53.1604
	Present (16×16)	SSSC	5.2387	90.2320	259.3216	10.6455
	Present (16×16)	SSSF	8.8427	240.5614	271.0575	14.8050
10	Present (16×16)	SSSS	8.926	20.3705	26.5258	1.3031
	Present (16×16)	SSCC	4.207	6.3735	27.2672	0.1290
	Present (16×16)	SSFF	9.220	21.2635	26.5537	0.4342
	Present (16×16)	SSSC	6.105	11.952	26.9187	1.1155
	Present (16×16)	SSSF	9. 098	20.8932	26.5432	1.3160

Table 7 Material properties at different temperatures $G_{13} = G_{12}$, $G_{23} = 0.5\ G_{12}$, $v_{12} = 0.3$, $\alpha_1 = -0.3 \times 10^{-6}$ and $\alpha_2 = 28.1 \times 10^{-6}$

Elastic moduli (GPa)	Temperatures T(K)					
	300	325	350	375	400	425
E_1	130	130	130	130	130	130
E_2	9.5	8.5	8.0	7.5	7.0	6.75
G_{12}	6.0	6.0	5.5	5.0	4.75	4.5

Table 8 Material properties at different moisture concentrations $G_{13} = G_{12}$, $G_{23} = 0.5\ G_{12}$, $v_{12} = 0.3$, $\beta_1 = 0$, and $\beta_2 = 0.44$

Elastic moduli (GPa)	Moisture concentrations C (%)						
	0	0.25	0.5	0.75	1.0	1.25	1.5
E_1	130	130	130	130	130	130	130
E_2	9.5	9.25	9.0	8.75	8.5	8.5	8.5
G_{12}	6.0	6.0	6.0	6.0	6.0	6.0	6.0

$$\overline{w} = \frac{w}{h\alpha_1 T_0 S^2}, \qquad (\overline{\sigma}_i, \overline{\tau}_{ij}) = \frac{(\sigma_i, \tau_{ij})}{E_1 \alpha_1 T_0}$$

The four layer anti-symmetric ($0^0/90^0/0^0/90^0$) cross-ply square laminate is analyzed with thickness ratios, ($S = a/h$) 100 and 10. In-plane normal stresses are calculated at the midpoint ($x = a/2$ and $y = a/2$), in-plane shear stress is calculated at the corner of the plate ($x = 0$ and $y = 0$) at thickness, $z = \pm\ h/2$. The results of non dimensional transverse displacement and in-plane stresses are presented in Table 6 under different boundary conditions, which are new results.

3.5 Response of laminated composite square plate ($0^0/90^0/0^0/90^0$) considering changes of material properties due to temperature and moisture variations

In previous studies, material properties of composite laminates are assumed to be independent of temperature/ moisture. However the elastic modulus of laminates in general is reduced with the elevated/increased temperature/ moisture. The change in material properties (Makhecha *et al.* 2001) due to change in temperature/ and moisture are shown in Tables 7 and 8 respectively. This example will illustrate the effect of changes in material properties due to change in temperatures/moisture on different structural responses.

In the first example, uniform rise of temperature ΔT at the top and bottom of the plate with in-plane sinusoidal variations is considered. The transverse displacement and in-plane stresses are presented in terms of following non-dimensional parameters

$$(\overline{\sigma}_x, \overline{\sigma}_y) = \frac{\sigma_x, \sigma_y}{\alpha_0 T_0 E_0}, \qquad \overline{w} = (w)/(\alpha_0 T_0)$$

Where $E_0 = 1$ GPa $T_0 = 300$ K, $\alpha_0 = 10^{-6}$ K^{-1}

Distribution of non-dimensional transverse displacement ($\overline{w}$) at the middle surface of a simply supported laminated
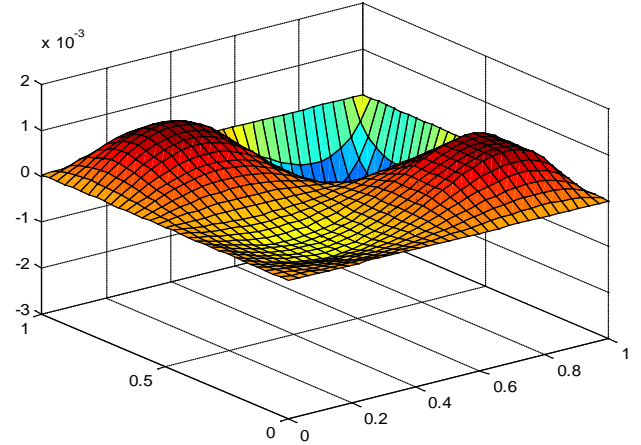

Fig. 3 Distribution of non-dimensional transverse displacement ($\overline{w}$) at the middle surface of laminated plate under uniform temperature ($0^0/90^0/0^0/90^0$, $a/h = 20$, $\Delta T = 350$ K)
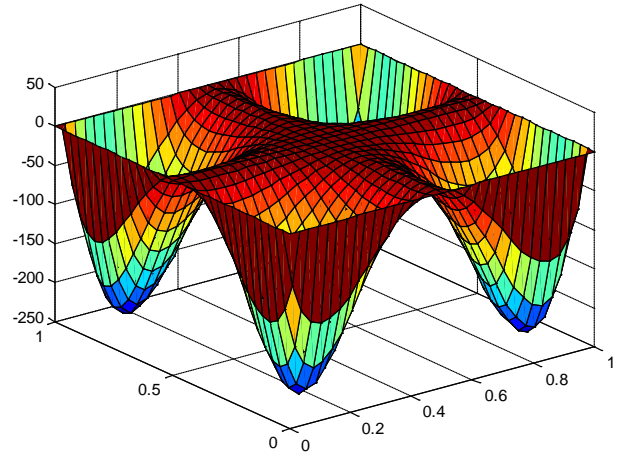

Fig. 4 Distribution of transverse displacement ($\overline{w}$) at the middle surface of laminated plate of eight layer under uniform moisture ($[0^0/90^0]_4$, $a/h = 10$, $\Delta C = 1.25\%$)

composite square plate ($0^0/90^0/0^0/90^0$) subjected to ($\Delta T = 350$ K) temperature with thickness ratio ($a/h = 20$) is plotted in Fig. 3.

In the second case, uniform rise of moisture concentration ΔC at the top and bottom of the plate with in-plane sinusoidal variations is applied. The non-dimen-sional transverse displacement is presented in the same manner as mentioned above.

Distribution of non-dimensional transverse displacement ($\overline{w}$) at the middle surface of a simply supported eight layer laminated ($0^0/90^0$)$_4$ composite square plate subjected to moisture concentration, $\Delta C = 1.25\%$ with thickness ratio ($a/h = 10$) is plotted as shown in Fig. 4.

All the above results are plotted above are new and are observed to follow the expected trend.

3.6 Buckling analysis of simply supported cross-ply laminated ($0^0/90^0/0^0$) composite plate

This problem is solved to assess the performance of the

Table 9 Normalized Critical buckling Temperature (λ_{cr}) for a simply supported square composite plate ($0^0/90^0/0^0$) for different thickness ratio (a/h)

a/h	References		
	Present	Matsunaga(2005)	Noor and Burton (1992)
100	0.9945×10^{-3}	0.9961×10^{-3}	0.9960×10^{-3}
20	0.2290×10^{-1}	0.2297×10^{-1}	0.2300×10^{-1}
10	0.7417×10^{-1}	0.7442×10^{-1}	0.7467×10^{-1}
5	0.1743	0.1752	0.1763
4	0.2126	0.2133	0.2148

present C⁰ FE model based on higher order zigzag theory in predicting the buckling behavior of a simply supported cross ply laminate subjected to uniform temperature rise in the *x-y* plane as well as through the thickness. The critical temperature (λ_{cr}) obtained for different thickness ratio (a/h) is shown in Table 9 by using the present FE model based on HZT. The present finite element results are observed to be very close to the results of 3D elasticity solution given by Noor and Burton (1992) as compared to the results of Matsunaga (2005) obtained by using a global higher order theory (Table 9). It is observed that critical buckling temperature increases with the decrease in thickness ratio. The corresponding material properties for the orthotropic plate are as follows

3.7 Vibration analysis of 10 layers simply supported angle-ply laminated composite square plates

This problem has been solved for a 10 layer angle-ply ($\theta = 15^0$) laminated composite plate with uniform temperature rise in the *x-y* plane as well as through the thickness. Normalized natural frequencies and critical temperatures obtained for different thickness ratio (a/h) using the present FE model based on different theories are shown in Table 9. The present results are in good agreement with the results obtained by Matsuanaga (2007). It is observed that results

obtained using present FE model based on HZT gives better results compared to results obtained by using HSDT. It is also observed that natural frequency increases with the decrease of thickness ratio (a/h). This trend is found in all subsequent examples in case of thermal vibration. The corresponding material properties for the composite plate are as follows

$$E_1/E_2 = 15, \quad G_{12} = G_{13} = 0.5E_2, \quad G_{23} = 0.3356E_2,$$
$$v_{12} = 0.3, \quad v_{23} = 0.49, \quad \alpha_1/\alpha_0 = 0.015, \quad \alpha_2/\alpha_0 = 1.0, \quad \rho = 1;$$

The normalized critical temperature is defined as follows: $\lambda_{cr} = \alpha_0 T$ where T is the critical temperature, α_0 is the normalization factor which is taken as 10^{-6}.

Normalized frequency is defined as follows $\Omega = \omega h\sqrt{\rho/E_2}$ where ω is the natural frequency, ρ is the density. The above normalization has been followed in the subsequent section.

4. Conclusions

In the present study, the static, buckling and vibration response of laminated composite plates exposed to hygrothermal environment is studied using an efficient C⁰ finite element model developed based on efficient higher order zigzag theory. The proposed model overcomes the problem of C¹ continuity associated with the presence of first derivatives of transverse displacement in the formulation by treating them as independent variables through C⁰ FE implementation and the number of nodal unknowns is lesser than the previous studies. Thus, the present FE model formulates a simple but accurate approach for the solution of different problems on laminated composite plates subjected to hygrothermal loadings. In order to remove the inconsistency between total strain and thermal strain special steps were introduced. Numerical results of static responses for different problems show that the proposed FE model for laminated composite

Table 10 Normalized natural frequency and critical temperature of a 10 layer angle-ply [θ/- θ/.../- θ]$_{10}$ square plate for different thickness ratio (a/h)

a/h	Theory	Ω		Theory	λ_{cr}	
		Present (12×12^1)	Matsunaga (2007)		Present (12×12^1)	Matsunaga (2007)
100	HZT	0.1336×10^{-2}	0.1328×10^{-2}	HZT	0.1123×10^{-2}	0.1161×10^{-1}
	HSDT	0.1335^{-2}		HSDT	0.1123^{-2}	
50	HZT	0.5306×10^{-2}	0.5286×10^{-2}	HZT	0.4419×10^{-2}	0.4600×10^{-2}
	HSDT	0.5301^{-2}		HSDT	0.4431^{-2}	
20	HZT	0.3208×10^{-1}	0.3302×10^{-1}	HZT	0.2533×10^{-1}	0.2700×10^{-1}
	HSDT	0.3227^{-1}		HSDT	0.2571^{-1}	
10	HZT	0.1163	0.1163	HZT	0.7894×10^{-1}	0.8899
	HSDT	0.1185^{+0}		HSDT	0.8251^{-1}	
5	HZT	0.3588	0.3592	HZT	0.1745	0.2124
	HSDT	0.3610		HSDT	0.1923	

[1] Mesh division

plates is capable in predicting results nearly close to the three dimensional elasticity solutions. The proposed FE model may, therefore, be recommended for wide use to generate further results for future research in the field.

References

Ali, J.S.M., Bhaskar, K. and Varadan, T.K. (1999), "A new theory for accurate thermal/mechanical flexural analysis of symmetric laminated plates", *Compos. Struct.*, **45**(3), 227-232.

Bahrami, A. and Nosier, A. (2007), "Interlaminar hygrothermal stresses in laminated shells", *Int. J. Solids Struct.*, **44**(25-26), 8119-8142.

Bhaskar, K., Varadan, T.K. and Ali, J.S.M. (1996), "Thermoelastic solutions for orthotropic and anisotropic composite laminates", *Compos.: Part B*, **27**(5), 415-420.

Brischetto, S. (2012), "hygrothermal loading effects in bending analysis of multilayered composite plates", *Comput. Model. Eng. Sci.*, **88**(5), 367-418.

Brischetto, S. (2013), "Hygrothermoelastic analysis of multi-layered composite and sandwich shells", *J. Sandw. Struct. Mater.*, **15**(2), 168-202.

Brischetto, S. and Carrera, E. (2010), "Coupled thermo-mechanical analysis of one-layered and multilayered plates", *Compos. Struct.*, **92**(8), 1793-1812.

Ebrahimi, F. and Habibi, S. (2016), "Deflection and vibration analysis of higher-order shear deformable compositionally graded porous plate", *Steel Compos. Struct., Int. J.,* **20**(1), 205-2225.

Hadji, L., Daouadji, T., Tounsi, A. and Bedia, E. (2014), "A higher order shear deformation theory for static and free vibration of FGM beam", *Steel Compos. Struct., Int. J.,* **16**(5), 507-519.

Kaci, A., Belakhdar, K., Tounsi, A. and Bedia, E.A.A. (2014), "Nonlinear cylindrical bending analysis of E-FGM plates with variable thickness", *Steel Compos. Struct., Int. J.,* **16**(4), 339-356.

Kant, T., Pandhari, S.S. and Desai, Y.M. (2008), "An efficient semi analytical model for composite and sandwich plates subjected to thermal load", *J. Therm. Stress.*, **31**(1), 77-103.

Kapuria, S. and Achary, G.G.S. (2004), "An efficient higher-order zigzag theory for laminated plates subjected to thermal loading", *Int. J. Solids and Struct.*, **41**(16-17), 4661-4684.

Khare, R.K., Kant, T. and Garg, A.K. (2003), "Closed-form thermo-mechanical solutions of higher-order theories of cross-ply laminated shallow shells", *Compos. Struct.*, **59**(3), 313-340.

Matsunaga, H. (2004), "A comparison between 2-D single layer and 3-D layerwise theories for computing interlaminar stresses of laminated composite and sandwich plates subjected to thermal loadings", *Compos. Struct.*, **64**(2), 161-177.

Nguyen, K.T., Thai, T.H. and Vo, T.P. (2015), "A refined higher-order shear deformation theory for bending, vibration and buckling analysis of functionally graded sandwich plates", *Steel Compos. Struct., Int. J.,* **18**(1), 91-120.

Lo, K.H., Christensen, R.M. and Wu, E.M. (1977a), "A high-order theory of plate deformation, Part 1: Homogeneous plates", *ASME J. Appl. Mech.*, **44**(4), 663-668.

Lo, K.H., Christensen, R.M. and Wu, E.M. (1977b), "A high-order theory of plate deformation, Part 2: Laminated plates", *ASME J. Appl. Mech.*, **44**(4), 669-676.

Lo, S.H., Wu, Z., Cheung, Y.K. and Chen, W. (2010), "Hygrothermal effects on multilayered composite plates using a refined higher-order theory", *Compos. Struct.*, **92**(3), 633-646.

Makhecha, D.P., Ganapathi, M. and Patel, B.P. (2001), "Dynamic analysis of laminated composite plates subjected to thermal/ mechanical loads using an accurate theory", *Compos. Struct.*, **51**(3), 221-236.

Matsunaga, H. (2005), "Thermal buckling of cross-ply laminated composite and sandwich plates according to a global higher-order deformation theory", *Compos. Struct.*, **68**(4), 439-454.

Matsunaga, H. (2007), "Free vibration and stability of angle-ply laminated composite and sandwich plates under thermal loading", *Compos. Struct.*, **77**(2), 249-262.

Naganarayana, B.P., Rama Mohan, P. and Prathap, G. (1995), "Quadrileteral C^0 laminated plate elements based on higher order transverse deformation theory", *Int. J. Eng. Anal. Des.*, **2**, 157-178.

Naganarayana, B.P., Rama Mohan, P. and Prathap, G. (1997), "Accurate thermal stress predictions using C^0 continuous higher-order shear deformable elements", *Comput. Methods Appl. Mech. Eng.*, **144**(1-2), 61-75.

Noor, A.K. and Burton, W.S. (1992), "Three-dimensional solutions for the thermal buckling and sensitivity derivatives of temperature–sensitive multilayered angle-ply plates", *Transact. ASME, J. Appl. Mech.*, **59**(4), 848-856.

Oh, J.H. and Cho, M.H. (2007), "Higher order zigzag theoryforsmart composite shell sunder mechanical–thermo-electric loading", *Int. J. Solids Struct.*, **44**(1), 100-127.

Ojalvo, I.V. (1974), "Improved thermal stress determination by finite element methods", *J. AIAA*, **12**(8), 1131-1132.

Pandit, M.K., Sheikh, A.H. and Singh, B.N. (2008), "An improved higher order zigzag theory for the static analysis of laminated sandwich plate with soft core", *Finite. Elem. Anal. Des.*, **44**(9-10), 602-610.

Patel, B.P., Ganapathi, M. and Makhecha, D.P. (2002), "Hygro-thermal effects on the structural behaviour of thick composite laminates using higher-order theory", *Compos. Struct.*, **56**(1), 25-34.

Pittr, J. and Hartl, H. (1980), "Improved stress evaluation under thermal load for simple finite element", *Int. J. Numer. Meth. Eng.*, **15**(10), 1507-1515.

Prathap, G. and Naganarayana, B.P. (1990), "Consistent force resultant distributions in displacement elements with varying sectional properties", *Int. J. Numer. Meths. Eng.*, **29**(4), 775-783.

Prathap, G. and Naganarayana, B.P. (1995), "Consistent thermal stress evaluation in finite elements", *Comput. Struct.*, **54**(3), 415-426.

Rama Mohan, P., Naganarayana, B.P. and Prathap, G. (1994), "Consistent and variationally correct finite elements for higher order laminated plate theory", *Composite Struct.,* **29**(3-4), 445-456.

Rolfes, R., Noor, A.K. and Sparr, H. (1998), "Evaluation of tranverse thermal stresses in composite plates based on first-order shear deformation theory", *Comput. Methods Appl. Mech. Eng.*, **167**, 355-368.

Savoia, M. and Reddy, J.N. (1995), "Three-dimensional thermal analysis of laminated composite plates", *Int. J. Solids Struct.*, **32**(5), 593-608.

Shankara, C. and Iyengar, N. (1996), "A C^0 element for the free vibration analysis of laminated composite plates", *J. Sound Vib.*, **191**(5), 721-738.

Singh, S.K. and Chakrabarti, A. (2011), "Hygrothermal analysis of laminated composite plates by using efficient higher order shear deformation theory", *J. Solid Mech.*, **3**(1), 85-95.

Topal, U. (2013), "Application of a new extended layerwise approach to thermal buckling load optimization of laminated composite plates", *Steel Compos. Struct., Int. J.,* **14**(3), 283-293.

Tungikar, V.B. and Rao, K.M. (1994), "Three-dimensional exact solution of thermal stresses in rectangular composite laminate", *Compos. Struct.*, **27**(4), 419-430.

Wang, X., Dong, K. and Wang, X.Y. (2005), "Hygrothermal effect on dynamic interlaminar stresses in laminated plates with piezoelectric actuators", *Compos. Struct.*, **71**(2), 220-228.

Wu, Z. and Chen, W. (2006), "An efficient higher-order theory and finite element for laminated plates subjected to thermal loading", *Compos. Struct.*, **73**(1), 99-109.

Wu, Z., Cheng, Y.K., Lo, S.H. and Chen, W. (2007), "Thermal stress analysis of laminated plates using actual temperature field", *Int. J. Mech. Sci.*, **49**(11), 1276-1288.

CC